

Near infrared adaptive optics imaging of high redshift quasars.

Renato Falomo

*INAF – Osservatorio Astronomico di Padova, Vicolo dell'Osservatorio 5, 35122 Padova,
Italy*

renato.falomo@oapd.inaf.it

Aldo Treves

Università dell'Insubria, via Valleggio 11, 22100 Como, Italy

treves@mib.infn.it

Jari K. Kotilainen

Tuorla Observatory, University of Turku, Väisäläntie 20, FIN-21500 Piikkiö, Finland

jarkot@utu.fi

Riccardo Scarpa

Instituto de astrofisica de Canarias, Spain

riccardo.scarpa@gtc.iac.es

and

Michela Uslenghi

IASF-CNR Milano, Via E. Bassini 15, Milano I-20133, Italy

uslenghi@mi.iasf.cnr.it

Received ... ; accepted ...

ABSTRACT

The properties of high redshift quasar host galaxies are studied, in order to investigate the connection between galaxy evolution, nuclear activity, and the formation of supermassive black holes. We combine new near-IR observations of three high redshift quasars ($2 < z < 3$), obtained at the ESO-Very Large Telescope equipped with adaptive optics, with selected data from the literature.

For the three new objects we were able to detect and characterize the properties of the host galaxy, found to be consistent with those of massive elliptical galaxies of $M_R \sim -24.7$ for the one radio loud quasar, and $M_R \sim -23.8$ for the two radio quiet quasars. When combined with existing data at lower redshift, these new observations depict a scenario where the host galaxies of radio loud quasars are seen to follow the expected trend of luminous ($\sim 5L^*$) elliptical galaxies undergoing passive evolution. This trend is remarkably similar to that followed by radio-galaxies at $z > 1.5$. Radio quiet quasars hosts also follow a similar trend but at a lower average luminosity (~ 0.5 mag dimmer). The data indicate that quasar host galaxies are already fully formed at epochs as early as ~ 2 Gyr after the Big Bang and then passively fade in luminosity to the present epoch.

Subject headings: Galaxies:active – Infrared:galaxies – Quasars:general – galaxies: evolution

1. Introduction

At low redshift quasars are hosted in otherwise normal luminous and massive galaxies (Bahcall et al. 1997; Hamilton et al 2002; Dunlop et al. 2003; Pagani et al. 2003) characterized by a conspicuous spheroidal component that becomes dominant in radio loud objects. These galaxies appear to follow the same relationship between bulge luminosity and mass of the central black hole (BH) observed in nearby inactive elliptical galaxies (Ferrarese 2006, for a recent review). If this link holds also at higher redshift the observed population of high z quasars traces the existence of $\sim 10^9 M_\odot$ super massive BHs and massive spheroids at very early (< 1 Gyr) cosmic epochs (Fan et al. 2001; Fan et al. 2003; Willott McLure & Jarvis 2003). This picture seems also supported by the discovery of molecular gas and metals in high z quasars (Bertoldi et al. 2003; Freudling Corbin & Korista 2003), that are suggestive of galaxies with strong star formation. In this context it is therefore important to push as far as possible in redshift the direct detection and characterization of QSO host galaxies. In particular, a key point is to probe the QSO host properties at epochs close to (and possibly beyond) the peak of quasar activity ($z \sim 2.5$).

Until few years ago, due to the severe observational difficulties, the properties of quasar host galaxies at high redshift were very poorly known (e.g. see the pioneering papers by (Hutchings 1995; Lehnert et al. 1992; Lowenthal et al. 1995), and uncertain or ambiguous results were produced because of inadequate quality of the images (modest resolution; low signal-to-noise data; non optimal analysis).

Deep images with adequate spatial resolution are essential. This goal is not easy to attain with HST because of its modest aperture that translates into a limited capability to detect faint extended nebulosity unless gravitationally lensed host galaxies are used (Peng et al. 2006). One has thus to resort to 10 meter class telescopes equipped with adaptive optics (AO) systems. This keeps the advantage of both high spatial resolution and high sensitivity although some complications are introduced: the need for a reference point source close to the target, and a time and position dependent point spread function (PSF). Moreover, unless artificial (laser) guide stars are available (not yet fully implemented in current AO systems) only targets which are sufficiently angularly close to relatively bright stars can actually be observed.

Though the first generation of AO systems at 4m class telescopes improved the detection of structures of the host at low z they did not allow much improvements for distant quasars (Hutchings et al. 1998; Hutchings et al. 1999; Marquez et al. 2001; Lacy et al. 2002; Kuhlbrodt et al 2003). Only very recently have AO imaging systems become available in large telescopes and could be used to image distant QSO with the full capability of spatial resolution and adequate deepness. Croom et al (2004) presented a study of 9 high z quasars imaged with the AO Gemini North telescope, but they were able to resolve only one radio quiet source at $z= 1.93$.

In order to investigate the properties of quasar hosts at $z > 2$ and explore the region near the peak of QSO activity we are carrying out a program to secure Ks band images of quasars in the redshift range $2 < z < 3$ using the AO system at ESO VLT. In a previous pilot work we presented the results for one radio-loud QSO (RLQ) (Falomo et al. 2005). Here we present new observations for three high z quasars, one RLQ and two radio quiet quasars (RQQ). Throughout this work we use $H_0 = 70 \text{ km s}^{-1} \text{ Mpc}^{-1}$, $\Omega_m = 0.3$, and $\Omega_\Lambda = 0.7$.

2. Object selection

Only targets sufficiently close to bright stars can be observed with adaptive optics systems employing natural guide stars as reference. Because of that, we searched the latest (Veron-Cetty & Veron 2006) AGN catalog (including data from the Sloan Digital Sky Survey and 2dF surveys (Schneider et al. 2003; Croom et al 2001)), for quasars in the redshift range $2 < z < 3$ and $\delta < 0$, having a star brighter than $V=14$ within 30 arcsec. Beside this bright source needed to close the AO loop, other stars in the field of view (FoV) are necessary in order to characterize the PSF, both in time and position on the field of view. Thus we required targets to have one or more stars in the FoV for PSF characterization. Under these conditions the AO system at the VLT is expected to deliver images of Strehl ratio better than ~ 0.2 when the external seeing is < 0.6 arcsec.

The twenty candidates fulfilling these requirements were then inspected individually looking at the Digitized Sky Surveys red plates. A priority was assigned according to the magnitude of the guide star and its distance from the target. Based on the allocated observing time we then chose one radio loud and 2 radio quiet objects (see Table 1).

3. Observations and data analysis

We acquired Ks-band images using NAOS–CONICA (Rousset et al. 2003; Lenzen et al. 2003), the AO system on the VLT at the European Southern Observatory (ESO) in Paranal (Chile). The CONICA used detector was Aladdin InSb (1024x1024 pixels) that provides a field of view of 56x56 arcsec with a sampling of 54 mas/pixel.

Each object was observed at random dithered positions, with small shifts applied between successive frames, within a jitter box of ~ 20 arcsec around the central position of the object, using individual exposures of 2 minutes per frame, for a total integration time of 38 min per observing block, each object had two observing blocks. The images (detailed in Table 1) were secured in service mode by ESO staff under photometric conditions. The accuracy of the photometric calibration, using standard stars observed during the same night, is of ± 0.1 mag.

Data reduction was performed by our own improved version of the ESO pipeline for jitter imaging data (Devillard 2001). It first corrects for bad pixels by interpolation from neighboring "good" pixels, and then applies flat fielding to each image, using a normalized flat field obtained by subtracting and averaging a number of ON and OFF images of the illuminated dome. The sky background level was evaluated and sky subtraction was obtained for each image using an appropriate scaling and median averaging of the temporally closest frames. The large number of raw frames and the size of the jitter width proved to be a robust procedure for generating reliable sky images from the science frames themselves. All

Table 1. Journal of the observations

| Quasar | Type | z | Date dd/mm/yy | V mag | Seeing " | FWHM " | Ks mag | GS(V,d) mag, " |
|----------------|------|-------|------------------|----------|-------------|-----------|-----------|-------------------|
| QSO 0020–304 | RQQ | 2.059 | 9/12/04 | 21.9 | 0.5 | 0.17 | 17.7 | 14.0, 18.5 |
| WGA 0633.1–233 | RLQ | 2.928 | 4/02/05 | 21.5 | 0.6 | 0.14 | 18.6 | 14.0, 22.3 |
| PKS 1041–0034 | RQQ | 2.494 | 30/01/05 | 20.7 | 0.6 | 0.15 | 18.4 | 14.5, 19.4 |

sky-subtracted images were then aligned to sub-pixel accuracy using 2-d cross-correlation of individual images using as reference all the point-like objects in the frames.

Data for each observing block were treated separately, thus we ended up with two combined images for each target. These were carefully compared and found to be very similar, thus we further co-added them to form a single image used for all the subsequent analysis.

Final modeling of the images was done with AIDA (Astronomical Image Decomposition and Analysis (Uslenghi & Falomo 2007; Uslenghi & Falomo 2007)), a software package specifically designed to perform two dimensional model fitting of QSO images, providing simultaneous decomposition into the nuclear and host galaxy components.

The most critical part of the analysis is the determination of the PSF model and the choice of the background level that affects the faintest external signal from the object.

3.1. PSF modeling

To model the PSF shape as a function of position in the FoV we used the image of the QSO 0633-23, that contains the largest number of stars. We first select those sources usable for PSF analysis on the basis of their full width at half maximum (FWHM), sharpness, roundness and signal-to-noise ratio, also including bright, slightly saturated stars useful to model the PSF faint wings. In total 14 stars were selected.

Each star was then modeled with a gaussian for the core and an exponential function for the wings. Regions contaminated by close companions, saturated pixels and other evident defects were masked out.

We found that both the FWHM and the ellipticity of the core component depend on the distance of the source from the guide star (see Figure 1). The FWHM ranges from 0.15 arcsec to ~ 0.3 arcsec while the ellipticity goes from 0.05 to 0.30 for objects close to the AO star and sources at ~ 40 arcsec, respectively. This analysis shows that the star most suited for PSF characterization should be at the same distance from the AO guide star as is the target. At distances from AO star < 30 arcsec the size of the PSF core is stable within 10 percent.

We found the major axis of the PSF core is oriented along the direction connecting the object with the star used for the AO correction (Fig. 1). On the contrary the shape of the wings is almost independent of the position in the field. This is expected in images obtained with AO corrections ((Tristram and Prieto 2005; Cresci et al. 2005)).

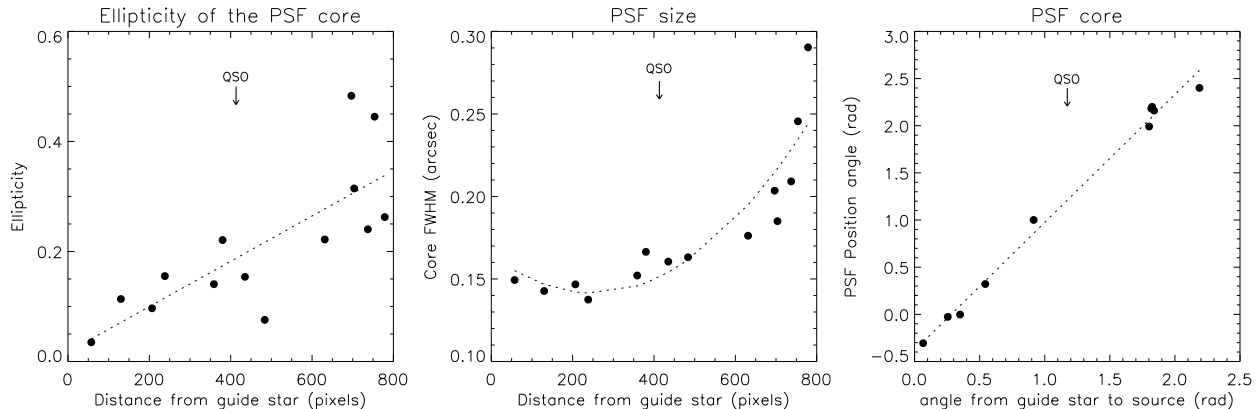


Fig. 1.— The first two panels show the variation of the PSF core properties with respect to the distance from the guide star. One pixel corresponds to 0.054 arcsec. The third (rightmost) panel shows the relation between direction of the elongation of the PSF core and the position angle of the line connecting the star with the guide star. In all panels the position of the target is indicated with QSO.

A map of the PSF differences with respect to the sharpest PSF was then created by fitting low order polynomial curves to the PSF parameters (Figure 1). This allowed us to evaluate the additional correction to be applied to the PSF model at the position of the target. The adopted PSF for the quasar was thus constructed using all the available stars in each frame and giving higher weight to those at similar distance from the AO star as the target.

The corrections map derived using the data for QSO 0633-23 was also used for the other two QSOs because of the limited number of stars available in these fields. Although some second order variations of the PSF cannot be excluded we are confident that the general trends are similar. Moreover the angular separation between AO guide star and PSF star is similar to the one between AO star and target (difference < 5 arcsec) thus the additional correction is very small and cannot affect the global result of our analysis.

3.2. QSO image decomposition

For each source, a mask was built to exclude contamination from other sources close to the target, bad pixels and other possible defects. In order to take into account possible small variations of the local background with respect to the overall zero level of the sky subtracted

images we computed the average signal in a circular annulus centered on the source and with radii of about 3-4 and 5-6 arcsec. We checked that in such annular regions the average radial brightness profile of the object remains flat and that the level of the signal inside the annular region was consistent in all cases with the level of the background measured outside this annular region. This ensures that in this region there is no extra extended emission due to the host galaxy or associated gas. The applied correction for the level of the local background allows us to properly evaluate the signal of the host galaxy in the very faint external regions. The amount of this correction is such that only the signal below surface brightness $\mu \sim 22.5$ (mag/arcsec²) is affected thus in all cases the objects would be resolved even without the correction.

The QSO images were first fitted using only the point source model in order to provide a first check of the deviation of the target from the PSF shape. If the residuals revealed a significant and systematic excess over the PSF shape, the object was fitted using a two component model (host galaxy plus a point source). Otherwise, the object was considered unresolved. In all three cases presented here it was found the object was resolved thus the final fit of the image of the target was obtained assuming it is composed of a point source and an elliptical or disc galaxy convolved with the proper PSF.

An estimate of the errors associated with the model parameters (magnitude of the nucleus, and magnitude and effective radius of the host) is shown in Figure 2. These uncertainties are consistent with those obtained using simulated quasars images (Uslenghi & Falomo 2007).

4. Results for individual objects

J002031-3041

This is a radio quiet quasar ($z = 2.059$) discovered in the 2dF survey (Croom et al 2001). Our Ks-band image (see Figure 3) shows the QSO close (6 arcsec) to a Ks = 13.3 star. The characterization of the PSF for this field is based on a bright (slightly saturated) star at about 6 arcsec from the target and by a couple of faint stars in the field. The core of the PSF was thus defined by the two faint stars while the external wing was constrained by the bright one (labeled PSF in Fig. 3). The PSF was then adjusted according to the distortion map computed using the data of WGA J0633.1-2333.

The comparison of the QSO and the PSF data shows a significant residual emission up to ~ 1.5 arcsec from the center (see Fig. 6) indicating that the object is resolved. The best 2-d modeling of this object yields a host galaxy with $M_R = -23.3$ and $R_e \sim 11$ kpc.

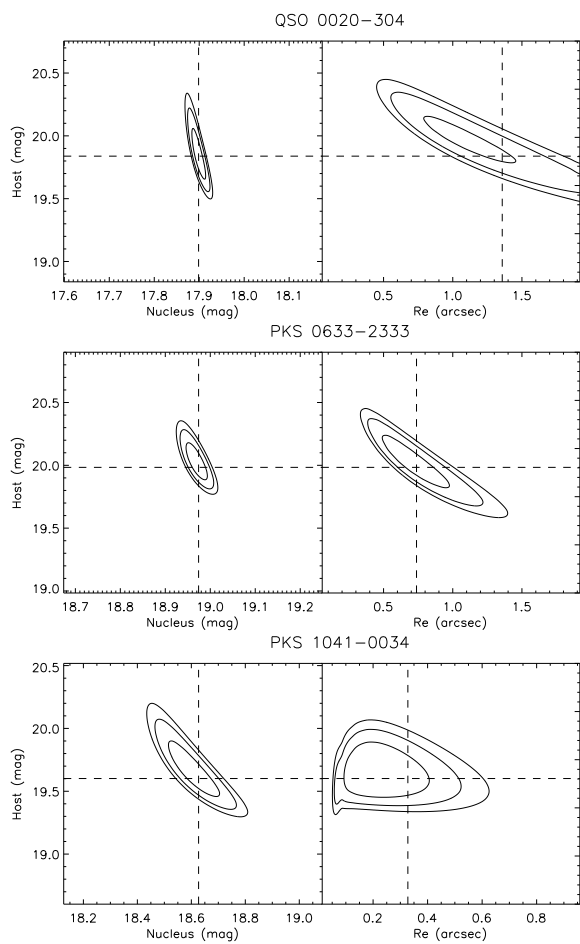


Fig. 2.— The χ^2 contour maps of the fit of the image of the objects as a function of the magnitude of the nucleus, host galaxy and the scale-length of the galaxy assuming an elliptical model. The three levels represent the confidence level probability of 68%, 95% and 99% from the inner to the outer region. The dashed lines show the best fit.

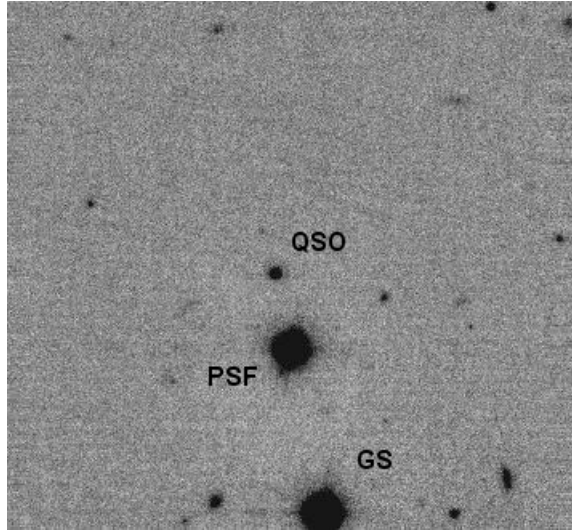


Fig. 3.— Ks-band image of the field of the QSO 0020-3041 obtained with VLT+NACO. The FoV shown is 40 arcsec; North is up and East to the left. The target (QSO), the guide star (GS) and the stars used for the characterization of the PSF are marked.

WGA J0633.1-2333

This radio loud quasar ($B = 21.5$) was discovered correlating the ROSAT WGACAT database with several radio catalogs ((Perlmann et al. 1998)). Its redshift $z = 2.928$ was derived from prominent emission lines of $\text{Ly}\beta + \text{OIV}$, $\text{Ly}\alpha$, and $\text{CIV } 1540 \text{ \AA}$ (Perlmann et al 1998). The luminosity of the quasar is $M_B = -24.6$. The 2-d decomposition (see Figure 6) shows the host galaxy has a disturbed morphology with an extended emission structure at ~ 0.5 arcsec East. Assuming an elliptical model the host galaxy properties are: $M_R = -24.65$ and $R_e \sim 6$ kpc.

J104117-0034

This radio quiet quasar ($V = 20.7$) was discovered in the 2dF survey (Croom et al 2001). The optical spectrum shows prominent $\text{Ly}\alpha$ and CIV emission lines at $z = 2.494$. No radio emission at 20 cm is detected in the FIRST survey at the position of the quasar.

The PSF was characterized using a star at a distance from the AO guide star similar to the distance between the AO guide star and the target (Fig. 5), also adjusted using the map derived from the WGA J0633.1-2333 data. Our analysis shows the object is resolved although we are not able to assess its morphology. Either an elliptical or a disk model for the

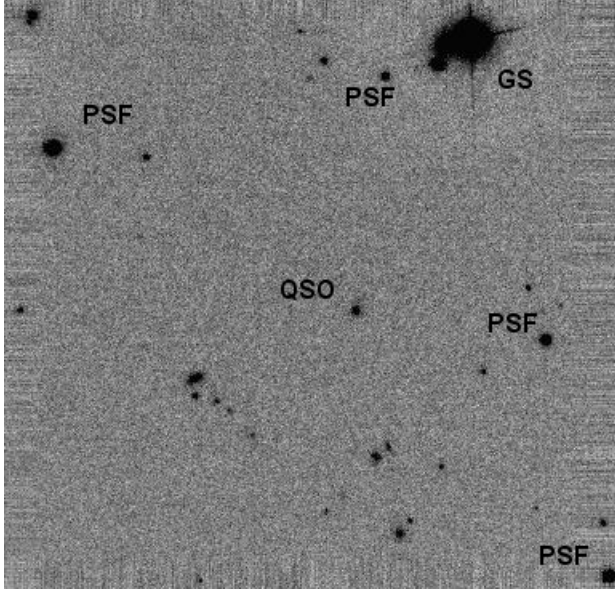


Fig. 4.— NACO Ks-band image of the radio loud quasar WGA J0633.1-2333. North is up and east to the left. The FoV is 40 arcsec. The target (QSO), the guide star (GS) as well as some stars used for characterization of the PSF are marked.

host galaxy can equally well fit the data. Under the assumption of an elliptical model the absolute magnitude of the host galaxy is $M_R = -24.1$ and the effective radius $R_e \sim 2.6$ kpc. If a disk model were assumed the host magnitude would be practically unchanged while the effective radius would be somewhat smaller.

Table 2. Results of image analysis

| Quasar | z | χ^2 | Ks(nuc) mag | Ks(host) mag | r_e " | K-cor Ks→R | R_e kpc | M_R (nuc) mag | M_R (host) mag |
|--------------|-------|----------|----------------|-----------------|------------|---------------|--------------|--------------------|---------------------|
| QSO 0020–304 | 2.059 | 0.33 | 17.9 | 19.8 | 1.4 | 3.05 | 11.3 | -25.2 | -23.2 |
| QSO 0633–233 | 2.928 | 0.47 | 19.0 | 20.0 | 0.7 | 2.75 | 5.7 | -25.0 | -24.3 |
| QSO 1041–003 | 2.494 | 0.90 | 18.6 | 19.6 | 0.3 | 2.93 | 2.6 | -25.0 | -24.0 |

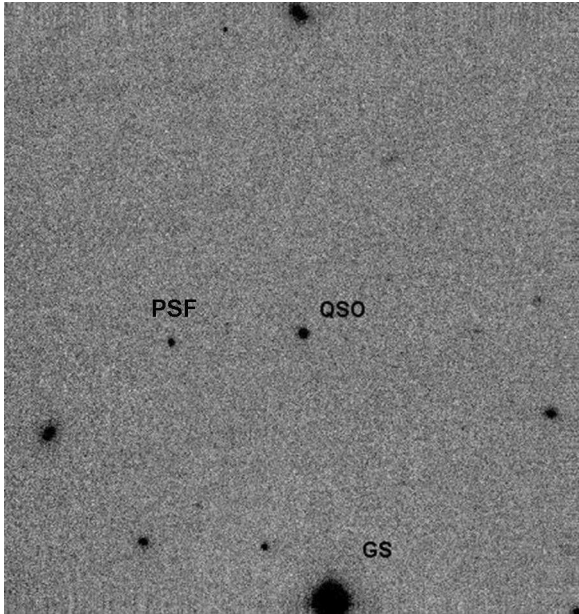


Fig. 5.— NACO Ks-band image of the radio quiet QSO J104117- 0034. North is up and east to the left. The FoV is 40 arcsec. The target (QSO), the guide star (GS) and stars used for characterization of the PSF are marked.

5. Discussion

To investigate the properties of the QSO hosts at different redshifts it is preferable to compare data probing the same rest frame wavelengths. The Ks band at $2 < z < 3$ closely matches the rest frame R band, thus in the following discussion our own data as well as data from the literature were transformed to the R band. This was done using the cross-band k-correction given in Tab. 2 with details given in the Appendix. This transformation is virtually independent of the assumed spectral energy distribution of the host galaxy over the whole redshift range of interest ($\Delta m < 0.2$ mag), allowing a reliable measurement of the rest frame luminosity.

In order to compare our results with those published in the literature at high redshift we considered only observations obtained in the NIR at large (8-10m class) telescopes or HST data. This allow us to perform a comparison of similar stellar populations detected in QSO host at lower z observed in the optical.

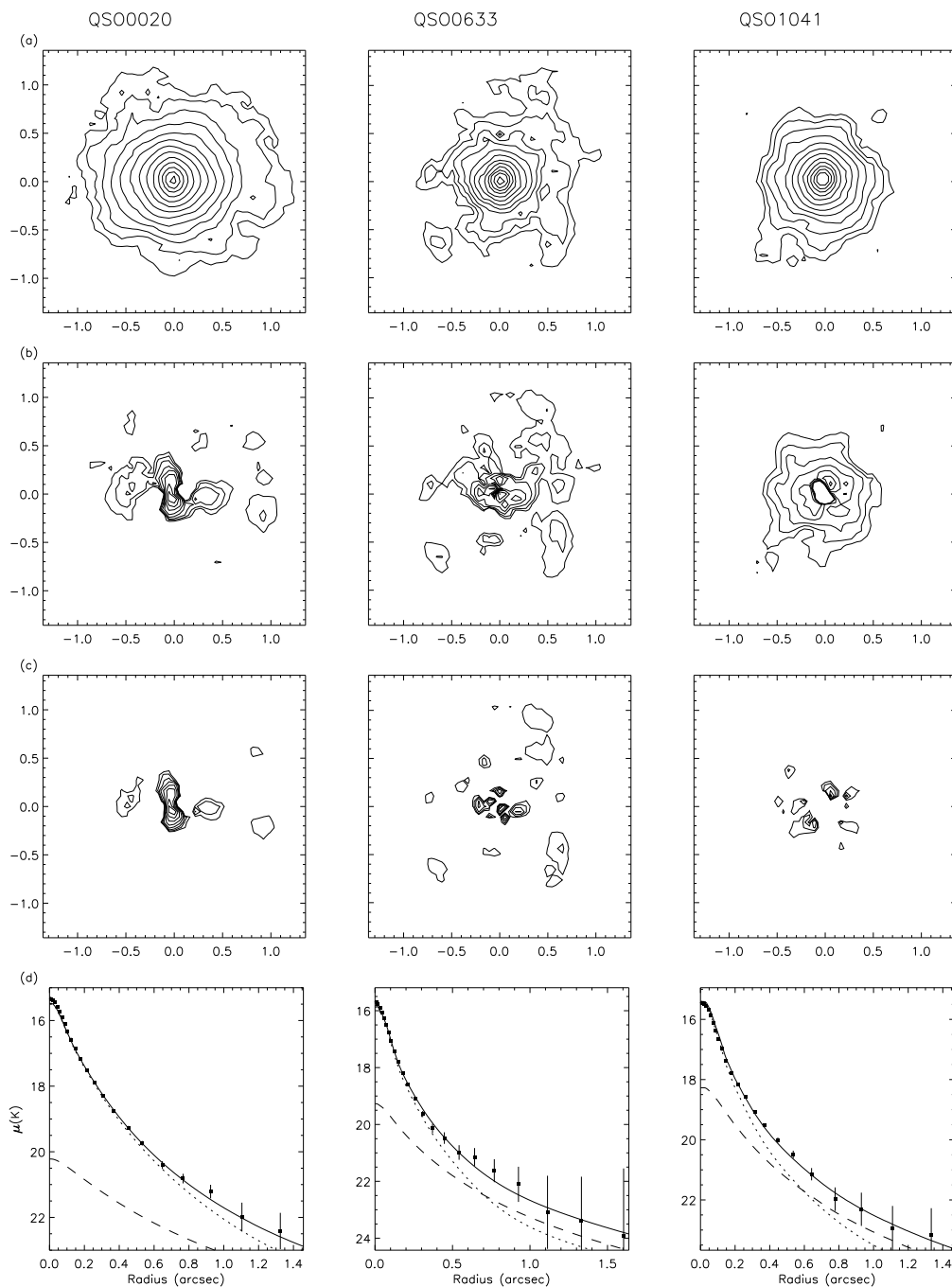


Fig. 6.— Contour plot of the object (top panel), object after subtraction of the PSF model (second from top), and residuals of the best fit (third from top). Scale of contour plots is in arcsec. Bottom panel: The radial surface brightness profile of the object (filled points) and the fitted model (solid line) with components (point source: dotted line; host galaxy: dashed line). The uncertainty in the radial surface brightness profile of the point source (PSF model) is about 0.1 mag at 0.5'' and 0.3 mag at 1.2''.

5.1. RLQs host galaxy evolution

In Figure 7 we report our new measurement for the host galaxy of one RLQ at $z \sim 3$, together with our previously reported RLQ hosts at $z = 2.55$ observed with VLT+ NACO (Falomo et al. 2005), and selected literature data. These include all results from HST WFPC2 images at $z < 0.6$, our previous survey of RLQ at $z < 2$ (Falomo et al. 2004; Kotilainen et al. 2007), and measurements of 4 objects by HST + NICMOS (Kukula et al. 2001). Two additional individual points at $z > 2$ were derived from the H mag of the host galaxy of lensed QSO reported by (Peng et al. 2006) transformed into R band following the method described above. All together these observations depict a general trend where the host luminosity increases by ~ 1.5 mag from present epoch up to $z \sim 3$. This is fully consistent with the expected luminosity evolution of a massive elliptical galaxy undergoing passive evolution. On average this trend corresponds to that of a galaxy of luminosity $\sim 5L^*$ (assuming $M^*(Ks) = -23.9$; (Gardner et al. 1997), corresponding to $M^*(R) = -21.1$) that is undergoing passive stellar evolution. The dominance of an old, evolved stellar population is also supported by spectroscopic studies of low redshift quasar (Nolan et al. 2001).

As mentioned above it is worth to note that this result is relatively robust with respect to the uncertainty for the filter transformation due to the choice of SED template for the galaxy since the comparison is done nearly at the same rest frame band. The only point that could move substantially is that at $z = 3.27$ (Peng et al. 2006) since it was observed in H band (see Appendix). In this case if instead of an elliptical model a Sb (or Sc) SED is assumed the host galaxy would be 0.4 (or 0.6) magnitudes fainter suggesting a possible drop of the host luminosity. With the caveat of the small statistics for RLQ hosts at high redshift we think that the present data do not show evidence for a drop in luminosity of RLQ hosts.

Several studies carried out at low redshift (Smith & Heckman 1989; Bettoni et al. 2001; Ledlow & Owen 1995) and high redshift (Willott McLure & Jarvis 2003; Inskip et al. 2005; Pentericci et al 2001; Zirm et al 2007) have shown that powerful radio emission is almost ubiquitously linked with massive and luminous ellipticals. Indeed the global photometric and structural properties of radiogalaxies are identical to those of non radio early type galaxies of similar mass (or luminosity). This is clearly apparent at low redshift since radiogalaxies follow the same fundamental plane of inactive normal ellipticals (Bettoni et al. 2001).

Given the above premises it is therefore of interest to compare the cosmic evolution of RLQ host luminosity with that of radiogalaxies (RG). (Willott McLure & Jarvis 2003) present a compilation of K band magnitudes of various samples of radiogalaxies. The observed K band magnitudes were converted to absolute M_R using the same transformations adopted for our objects. Then we have binned the data into redshift intervals of $\Delta z = 0.3$ from $z = 0$ to $z = 2$ and of $\Delta z = 0.5$ at $z > 2$. The trend in luminosity of this dataset of radio-

galaxies is very similar to that exhibited by the host of RLQ (see Figure 7). At $z < 1$ there is a small systematic difference (by ~ 0.5 mag) in the luminosity evolution between RLQ hosts and RG. This is difficult to interpret because of the non homogeneous definition of the RG dataset (compilation from various different surveys, (Willott McLure & Jarvis 2003)) can introduce selection effects in the RG samples.

Nevertheless it is remarkable that both RG and RLQ hosts follow a similar trend of the luminosity up to redshift $z \sim 3$. In our opinion this is suggestive of a common origin of the parent galaxies and also emphasizes that both types of radio loud galaxies follow the same evolutionary trend of inactive massive spheroids. This result can be seen also in the conventional K-z plot comparing radio galaxies and QSO hosts at $z > 1$ (see Figure 8). A similar scenario was found by (Hutchings 2006) for a small sample of higher z quasars.

5.2. RQQs host galaxy evolution

Since the hosts of RQQ are on average less luminous than those of RLQ their study at high redshift is more difficult. Indeed very little is known at $z > 2$. In Figure 9 we report our new detections for two radio quiet quasar hosts at $z > 2$ compared with data from the literature at lower redshift (Dunlop et al. 2003; Kukula et al. 2001; Hyvonen et al 2007; Falomo et al. 2004; Kotilainen et al. 2007 ; Croom et al. 2004).

With the possible exception of the RQQ at $z \sim 1.9$ detected by (Croom et al. 2004) the host galaxy luminosity of RQQs appears to increase by about 1 mag from $z=0$ to $z \sim 2.5$. This is consistent with the trend for non-active massive elliptical galaxy of $M = M^* - 1$ undergoing simple passive evolution. This is also similar to the behavior observed for RLQs hosts but occur on average at a lower level of luminosity (about 0.5 mag fainter). Moreover it is worth to note that the same level of luminosity corresponds to that of non-active early type galaxies at $z \sim 1.4$ (Longhetti et al 2007) and at $z \sim 1.8$ (Daddi et al 2005).

(Peng et al. 2006) report the detection of the host galaxy of a number of gravitational lensed quasars without radio classification, 8 in the redshift range $2 < z < 3$ and 1 at $z > 3$. Considering that the vast majority of QSO are radio quiet, one might assume that most of them are RQQ. Under this assumption and after converting their H band host luminosity to R band rest frame according to our SED galaxy template, we found their luminosity ($\langle M_R \rangle$

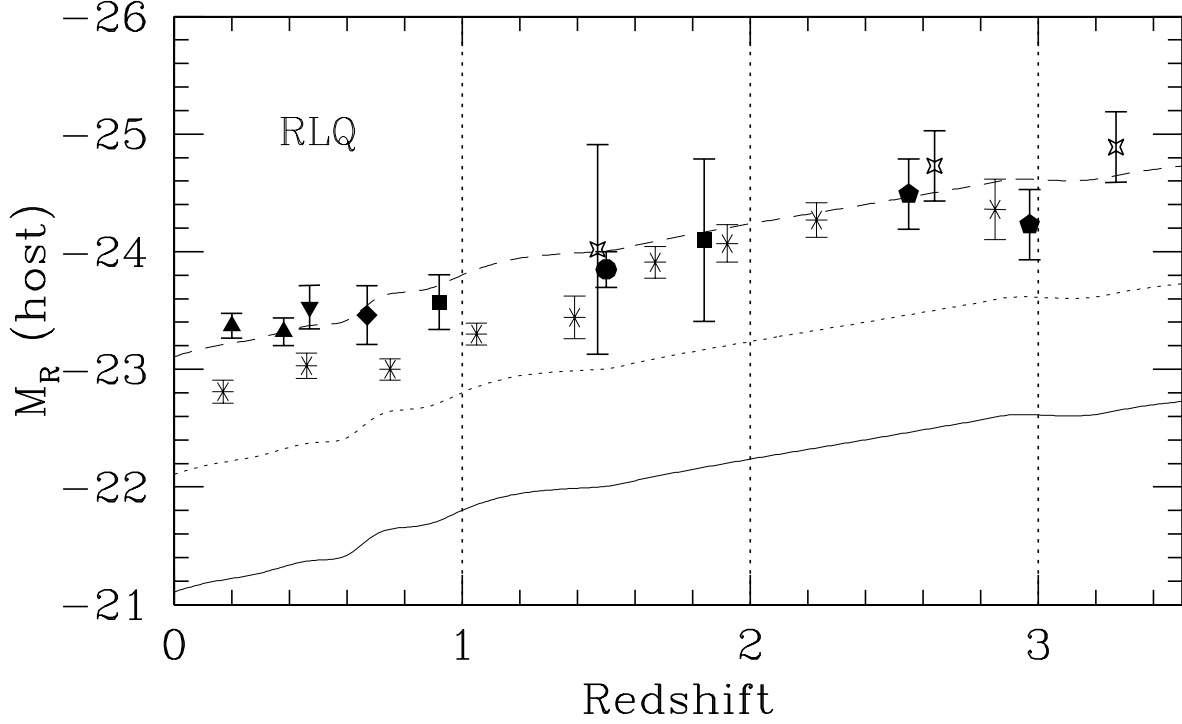


Fig. 7.— The evolution of radio loud quasar host luminosity compared with that expected for massive ellipticals (at M^* , M^*-1 and M^*-2 ; *solid*, *dotted* and *dashed* line) undergoing passive stellar evolution (Bressan Granato & Silva 1998). The host galaxy of the RLQ at $z \sim 2.9$ presented in this work, and another RLQ at $z \sim 2.5$ from (Falomo et al. 2005) are shown as filled pentagons. Other symbols represent: HST observations by (Dunlop et al. 2003) and (Pagani et al. 2003) (triangles), (Hooper et al. 1997) (inverted triangles); (Kukula et al. 2001) (squares); ESO NTT observations (Kotilainen & Falomo 2000) (diamond). VLT observations (Falomo et al. 2004) and (Kotilainen et al. 2007) (circle); HST data for lensed hosts by (Peng et al. 2006) (open stars). Each point is plotted at the mean redshift of the sample with error bars representing the 1σ dispersion of the sample. In the case of individual objects the uncertainty of the measurement is given. A binned version of the data for radio galaxies shown in Fig. 8 is also given (asterisks).

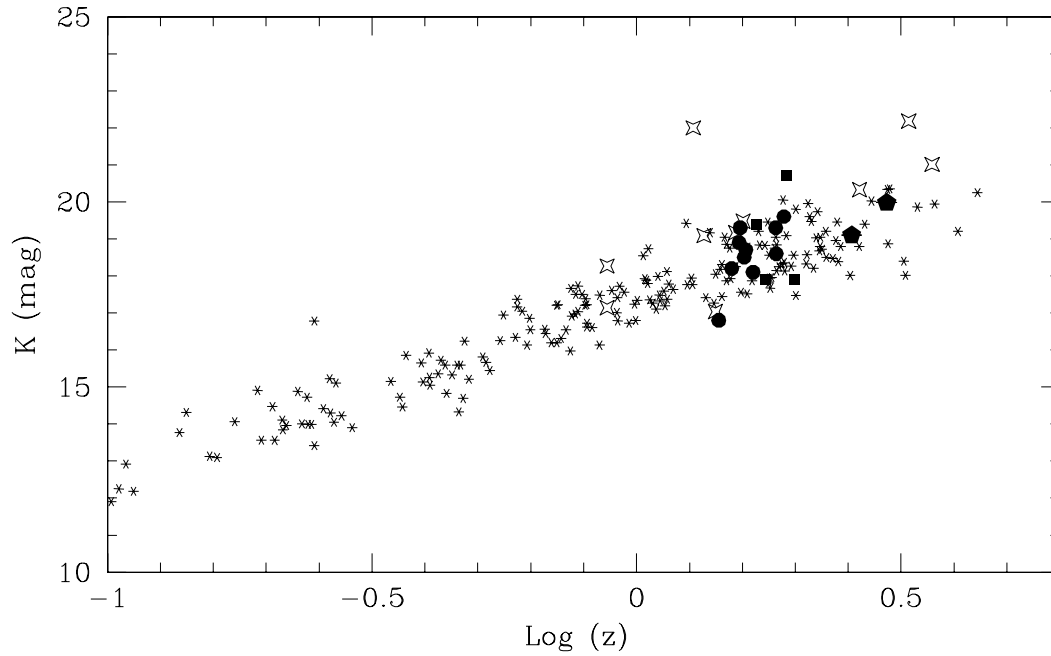


Fig. 8.— Apparent K band magnitude versus redshift (the K-z plot) for luminous radio-galaxies (asterisks) ((Willott McLure & Jarvis 2003) compared with host of RLQ at $z > 1$. Symbols represent VLT data by (Falomo et al. 2004) and (Kotilainen et al. 2007) (circles); HST data by (Kukula et al. 2001)(squares); HST data of gravitational lensed QSO by (Peng et al. 2006) (open stars). The two radio loud QSO presented in this work are also shown (pentagons).

$= -24.8$ at $\langle z \rangle \sim 2.5$; $M_R = -25.4$ at $z \sim 3.4$) is well above the overall trend drawn by the objects at lower redshift. The only point that could be significantly affected by the choice of the SED is the individual source at $z \sim 3.4$ that, in the case of an Sb template, would be fainter by 0.7 mag. In any case the (Peng et al. 2006) data for these high z QSO hosts appear well separated from the objects at lower redshift.

Note that the average value of Peng et al. data in the range $1 < z < 2$ are fully consistent (see Figure 9) with our extensive previous study performed at VLT (Falomo et al. 2004; Kotilainen et al. 2007) thus no systematic effects due to different analysis are expected. One possibility to explain this difference of host average luminosity at $z > 2$ is that some (or most) of these objects are radio loud and thus their host would be naturally brighter. However, this may be difficult to assess because they are lensed objects. Another possibility is that since the objects at $z > 2$, studied by Peng et al., have quite luminous nuclei (average $\langle M_B \rangle = -26$) also their host galaxies could be systematically more luminous than those in the rest of QSO samples ($M_B \sim -24.3$ for our RQQ at $z > 2$).

Detection of extended emission in the near-IR has been also found for QSO at very high redshift by (Hutchings 2003). This paper reports Gemini North direct images secured under average conditions (seeing 0.7 arcsec) for 5 QSO at $z \sim 4.7$. The observed K band host magnitude for these objects (as estimated from PSF removal and extrapolated flux profile) are in the range $K_s = 19.3$ to 20.5 . This corresponds to R band absolute magnitudes in the range $M(R) = -26.6$ to -27.8 assuming an elliptical galaxy SED or ~ 0.5 mag fainter in the case of disk galaxy SED. In both cases these data compared with those presented in our paper show these host galaxies are substantially more luminous (by a factor at least 5) than the trend derived from the whole dataset up to $z \sim 3$. However it is worth to note that at this redshift the K band is mapping the host galaxy at $\sim 3700 \text{ \AA}$. Therefore the stellar population responsible for the observed emission is very different from that considered in the rest of the dataset (rest frame R or I). If such high luminosity will be confirmed at high z it may indicate a substantial amount of star formation at these epochs.

Finally we comment on the very recent and intriguing result by (Schramm et al 2007) of 3 RQQ at $z = 2.6-2.9$, that appear to have host galaxies of extremely high luminosity ($M_R(\text{host}) = -25.8$ to -26.8). They are at least 3 magnitudes above M^* after including passive evolution. These results are very difficult to reconcile with the rest of quasar host detection at similar or lower redshift and would imply exceedingly high ongoing star formation. Given the scanty information on these luminous high z QSO it is not clear if these are exceptional cases possibly associated with very high luminous quasars.

As a whole, with the caveat that at $z > 2$ there are only few measurements and large differences among objects, the present observations do not exhibit any signature of a drop

in luminosity (or mass) of the RQQ hosts up $z \sim 2.5$.

6. Conclusions

The main motivation of this paper is to contribute to the measurement of the stellar luminosity of the host galaxy of high z quasars, which is a probe of the host galaxy mass. As a whole, while not excluding the possibility in some cases of ongoing episodes of star formation, the available data are consistent with no evolution in mass, indicating therefore that QSO host galaxies are already well formed at $z \sim 3$. Since then they passively fade to the present epoch. This is at odds with one of the main conclusion by (Peng et al. 2006).

This has important implications for theories of the structure formation in the Universe. In particular hierarchical merging scenarios predicting a substantial mass reduction at early epochs (Kauffmann & Haehnelt 2000), as well as those models predicting a late merging and assembly period for local massive spheroids, have difficulties in explaining the existence of a substantial population of massive, passive (red and dead) early-type galaxies at high redshift (e.g. McCarthy et al. 2004, Cimatti et al 2004, (Daddi et al 2005; Papovich et al 2006; Longhetti et al 2007)). Only the most recent hierarchical models (e.g. (Granato et al 2004; De Lucia et al 2005; Croton et al 2006; Bower et al 2006) which take into account the influence of the central supermassive black hole (AGN feedback, e.g. through heating of gas in massive halos by AGN energetic), do in fact agree reasonably well with the observed stellar mass function and allow for the existence of massive early-type galaxies out to $z \sim 4$.

Our results have important implications also for the study of the parameter $\Gamma = (M_{BH}/M_{sph})$, linking black hole and host galaxy masses (e.g. (Merloni et al 2006)). For a sample of ~ 30 quasars at $z \sim 0.3$ (Labita et al. 2006) found Γ is consistent with the value for quiescent galaxies in the local Universe, confirming an earlier result reported by (McLure & Dunlop 2001) for a different sample of low z quasars. On the other hand, a decreasing Γ was derived from a study of a sample of Seyfert galaxies at $z \sim 0.36$ (Treu et al 2007). At high z the situation is even less clear. In their study of gravitationally lensed quasar from the CASTELS-HST project (Peng et al. 2006) claim Γ is consistent with the local value up to $z = 1.7$. After that, Γ sharply increases by a factor 4. Our results strongly suggest the mass of the host galaxy does not significantly change with the cosmic time (at least up to $z \sim 3$). At face value the claim by Peng et al. would then imply the untenable scenario where M_{BH} is decreasing with the cosmic time. See however

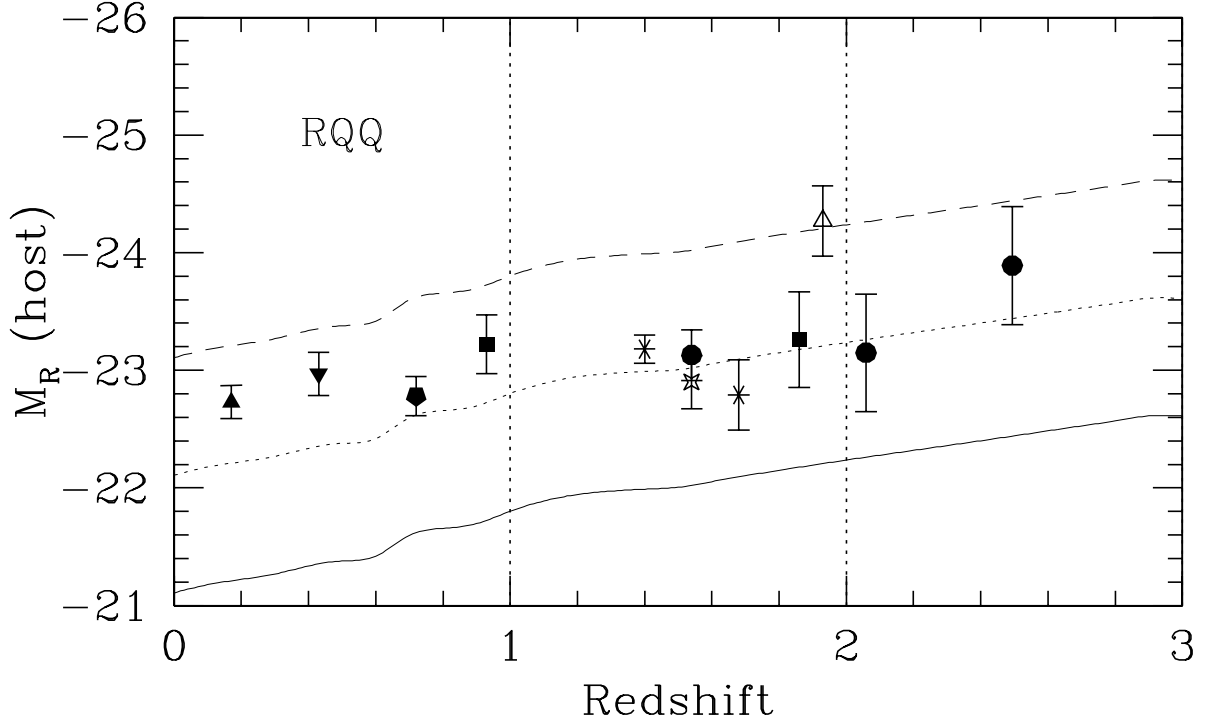


Fig. 9.— The evolution of radio quiet quasar host luminosity compared with that expected for massive ellipticals (at M^* , M^*-1 and M^*-2 ; *solid*, *dotted* and *dashed* line, respectively) undergoing passive stellar evolution (Bressan Granato & Silva 1998). The two new RQQ at $z \sim 2.05$ and 2.5 presented here are marked with filled circles. The data for samples at lower redshift are: (Dunlop et al. 2003) and (Pagani et al. 2003, triangles); (Hooper et al. 1997) (inverted triangle) ; (Kukula et al. 2001, squares); (Hyvonen et al 2007, pentagons); (Falomo et al. 2004) and (Kotilainen et al. 2007)(circle); (Croom et al. 2004) (open triangle) ; (Peng et al. 2006) (open stars) ; see also (Falomo et al. 2004) for details on previous samples. Crosses represent the luminosity of massive early type galaxies at $z \sim 1.4$ and $z \sim 1.8$ studied by (Longhetti et al 2007) and (Daddi et al 2005), respectively. Each point is plotted at the mean redshift of the sample with error bars representing the 1σ dispersion of the sample. In the case of individual objects the uncertainty of the measurement is given.

(Lauer et al. 2007) for the possible presence of selection bias affecting the samples considered by (Peng et al. 2006) and (Treu et al 2007). It is also worth to note the very high luminosities reported by (Peng et al. 2006) for a number of alleged RQQ host galaxies at $z > 2$ implies an higher luminosity with respect to the passive evolution. If confirmed this would exacerbate the problem of the M_{BH} dependence on z implied by Γ .

Because of the potential cosmological importance of the result in the context of the models of galaxy and SBH formation it is mandatory to resolve a sizeable number of objects at $z \sim 3$ and beyond. These observations should be done in the K band in order to minimize the uncertainty on the k-correction due to the assumed SED of the objects.

7. Appendix - Cross filter k-correction

We have trasformed Ks magnitudes into rest frame R along the lines described in (Hogg et al 2002). To perform this transformation we assumed the SED for an elliptical galaxy (Mannucci et al. 2001) and compared the integrated flux through the standard R (Cousins) filter to that in Ks band taking into account both the different zero point calibration and the wavelength stretching effect by $(1+z)$.

In Figure 10 we report the conversion from the observed H and Ks magnitudes to rest frame R band for three different galaxy SED models (Elliptical, Sa and Sc) taken from (Mannucci et al. 2001). In the conversion between Ks to R the uncertainty associated to the choice of the SED of the galaxy is less than 0.2 mag for the whole redshift range considered here (from $z = 0$ to $z = 4$). A similar uncertainty is found for the correction between H and R up to $z = 2.5$, while beyond this limit the different choice of SED lead to substantial different corrections up to 1 mag at $z = 3.5$.

Acknowledgments

This work was partially supported by PRIN 2005/32. This research has made use of the NASA/IPAC Extragalactic Database (*NED*) which is operated by the Jet Propulsion Laboratory, California Institute of Technology, under contract with the National Aeronautics and Space Administration. This work was supported by the Academy of Finland (project 8107775)

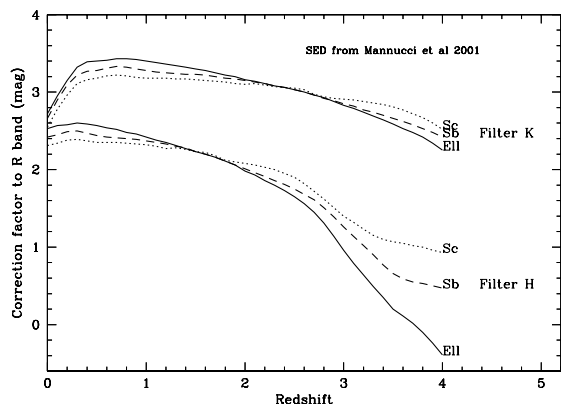


Fig. 10.— The cross filter correction between H (bottom curves) and Ks (top curves) observed magnitudes at various redshift to the magnitude in R band at rest frame. Three different SED galaxy models are considered : Elliptical (solid line); Sb (dashed line); Sc (dotted line). Spectral templates are drawn from (Mannucci et al. 2001)

REFERENCES

- Bahcall, J.N., Kirhakos S., Saxe D.H., Schneider D.P. 1997, ApJ 479, 642
- Bettoni, D., Falomo, R., Fasano, G., Govoni, F., Salvo, M. & Scarpa, R. 2001, A&A, 380, 471
- Bertoldi F., Carilli C.L., Cox P., et al. 2003b A&A 406, L55
- Bower G.C. et al 2006 MNRAS 370 645
- Bressan, A., Granato G.L. & Silva L. 1998, A&A 332, 135.
- Cimatti A. et al 2004 Nature 430 184
- Cresci, G. Davies, R. I. Baker, A. J. Lehnert, M. D. 2005 A&A 438 757
- Croom S.M., Smith R.J., Boyle B.J., Shanks T., Loaring N.S., Miller L., Lewis I.J. 2001 MNRAS 322, L29
- Croom S.M., Schade D., Boyle B.J., Shanks T., Miller L., Smith R.J. 2004 ApJ 606 126
- Croton D.J. et al 2006 MNRAS 367, 864
- De Lucia G. et al 2005 MNRAS 366,499.
- Daddi E. et al 2005 ApJ 626 680

- Devillard, N. 2001 in *Astronomical Data Analysis Software and Systems X*, ASP Conf. Ser., 238, 10, 525
- Dunlop, J.S., McLure, R.J., Kukula, M.J., Baum, S.A., O’Dea C.P., Hughes, D.H. 2003, *MNRAS*, 340, 1095
- Falomo, R. Kotilainen, J.K., Pagani, C. Scarpa R. & Treves A. 2004, *ApJ* 604 495
- Falomo, R. Kotilainen, J.K., Scarpa R. & Treves A. 2005, *AA* 434 469
- Fan X. et al. 2001, *AJ*, 121, 54
- Fan X. et al. 2003, *AJ*, 125, 1649
- Ferrarese, L., 2006, in "Joint evolution of black holes and galaxies" Eds. M. Colpi et al. Taylor and Francis, NY, London.
- Freudling W., Corbin M.R., & Korista K.T. 2003 *ApJ* 587, 67
- Granato G.L. De Zotti G. Silva L., Bressan A., Danese L., 2004 *Apj* 600 580
- Gardner, J. P. Sharples, R. M. Frenk, C. S. Carrasco, B. E. 1997 *ApJ* 480 L99
- Hamilton T.S., Casertano S., Turnshek D.A., 2002, *ApJ*, 576, 61
- Hogg, D.W. Baldry, I.K. Blanton, M.R. Eisenstein, D.J. 2002 (arXiv:astro-ph/0210394)
- Hooper, E.J., Impey C.D. & Foltz C.B., 1997, *ApJ*, 480, L95
- Hutchings, J. B. 1995 *AJ*, 110, 994
- Hutchings J.B. Crampton D., Morris S.L., Steinbring E. 1998 *PASP* 110 374
- Hutchings J.B., Crampton D., Morris S.L., Durand D., Steinbring E., 1999 *AJ* 117, 1109
- Hutchings, J.B. *AJ* 125 1053
- Hutchings, J.B. 2006 *NewAR* 50 685
- Hyvonen T., Kotilainen, J.K., Orndhal, E. , Falomo, R. 2007 *AA* 462 525
- Inskip, K.J., Best P.N., Longair M.S. Rottgering H.J.A. 2005 *MNRAS* 359 1393
- Juneau S. et al 2005 *ApJ* 619, 135
- Kauffmann, G., Haehnelt, M., 2000, *MNRAS*, 311, 576

- Kotilainen, J.K., Falomo, R. 2000, A&A, 364, 70
- Kotilainen, J.K., Falomo, R., Labita, M., Treves, A. & Uslenghi, M. 2007, ApJ 660 1039
- Kuhlbrodt B., Oerndahl E., Wisotzki L., & Jahnke K. 2005 AA 439 497
- Kukula M.J., Dunlop J.S., McLure R.J., Miller L., Percival W.J., Baum S.A
- Labita M. Treves A. Falomo R Uslenghi M. 2006 MNRAS 373 551
- Lacy M., Gates, E.L. Ridgway, S.E., de Vries W. Canalizo G., Lloyd, J.P., Graham, J. R.
2002 AJ 124 3023
- Lauer T.R. Tremaine S. Richstone D. Faber S.M. 2007 arXiv/0705.4103
- Lehnert, M.D., Heckman, T.M., Chambers, K.C., Miley, G.K. 1992 ApJ, 393, 68
- Lenzen R., Hofmann R., Bizenberger P., Tusche, A., 2003, Proc. SPIE, 4841, 944
- Ledlow, M.J., & Owen, F.N. 1995 AJ, 110, 1959
- Longhetti, M. et al MNRAS 374 614
- Lowenthal, J.D., Heckman, T.M., Lehnert, M.D., Elias, J.H. 1995 ApJ, 439, 588
- Mannucci F. et al. 2001 MNRAS 326, 745
- Marquez I., Petitjean P., Thodore B., Bremer M., Monnet G., Beuzit J.-L. 2001 AA 371 97
- McLure R.J., Dunlop J.S., 2001, MNRAS, 327, 199
- McCarthy T.J. et al. 2004 ApJ 614 L9
- Merloni, A. Rudnick G., Di Matteo T. 2006 astro-ph/0602530.
- Nolan et al. 2001 MNRAS 323, 308
- Pagani, C., Falomo, R., Treves, A., 2003, ApJ 596, 830
- Papovich C. et al 2006 ApJ 640, 92.
- Peng C.Y. et al 2006 ApJ 649 616
- Pentericci L., McCarthy P.J., Roettgering H.J.A, Miley G.K., van Breugel W.J.M., Fosbury
R. 2001 ApJS 135 63
- Perlmann E., Padovani, P. Giommi P. et al. 1998AJ 115 125.

- Poggianti, B.M., 1997, A&AS, 122, 399 Proc. SPIE, 4007, 72
- Rousset, G., Lacombe, F., Puget, P., Gendron, E., Arsenault, R., et al., 2003, Proc. SPIE, 4839, 140
- Schneider D.P. Fan X., Hall P.B., Jester S., Richards G.T., Stoughton C., Strauss M.A., Subbarao M., Vanden Berk D.E., Anderson S.F., et al. 2003, AJ, 126, 2579
- Schramm M. Wisotzki L. Jahnke K. 2007 astroph/0709.2568
- Smith, E.P.& Heckman, T.M., 1989, ApJ, 341, 658
- Tristram, Konrad R. W.; Prieto, M. Almudena 2005: Science with Adaptive Optics Proceedings of the ESO Workshop Held at Garching, Germany, 16-19, Springer-Verlag Berlin/Heidelberg
- Treu, T., Woo, J-H, Malkan, M. A., Blandford, R. D. astro-ph/0706.0519
- Uslenghi M. & Falomo, R. 2007, Proc. Erice Apr 2007 in press.
- Uslenghi M. & Falomo, R. 2007, in preparation
- Veron-Cetty M.P., Veron P. 2006, A&A, 455, 773
- Willott C.J., Rawlings, S., Jarvis M.J. & Blundell, K. M. 2003 MNRAS 339 173
- Zirm et al 2007 ApJ 656 6